Exploration of Coriolis force on motion of air over the upper horizontal surface of a paraboloid of revolution

O K Kọríkọ[1], **K S Adegbie**[1], **A S Oke**[1,2] **and I L Animasaun**[1,3]

[1] Department of Mathematical Sciences, Federal University of Technology, Akure, Nigeria
[2] Department of Mathematical Sciences, Adekunle Ajasin University, Akungba Akoko, Nigeria

E-mail: okkoriko@futa.edu.ng, ksadegbie@futa.edu.ng, okeabayomisamuel@gmail.com and ilanimasaun@futa.edu.ng

CrossMark

Abstract

The significance of Coriolis force on the flow of air across a surface in rotating frame of reference is of prime importance in Astrophysics, Stellar dynamics, oceanography, meteorology and dynamo theory by influencing the movement of fluid upon the surface of the Earth. Sequel to the importance of Newtonian fluids (i.e. air and water), it is worthwhile to investigate the influence of Coriolis force on such flow. This is necessary due to the fact that Coriolis force is the only explanation for how the air heated by the Sun reaches the Earth. The significance of rotational force on the flow of Newtonian fluids over an upper horizontal surface of a paraboloid of revolution is investigated. The flows are modeled by incorporating the Coriolis term into the body forces of Navier–Stokes equations to obtain appropriate equations for the fluids. The governing equations is nondimensionalized using appropriate Blasius similarity variables to reduce the nonlinear partial differential equations to nonlinear ordinary differential equations. The resulting system of nonlinear ordinary differential equations is solved using Runge–Kutta–Gills method with Shooting technique and the results is depicted graphically. With an increase in Coriolis force, the horizontal velocity, the vertical velocity and the shear stress near the wall decrease while the temperature distribution is an increasing property.

Keywords: motion of air, coriolis force, heat transfer, fluid flow, boundary layer flow

(Some figures may appear in colour only in the online journal)

1. Introduction

1.1. Background information

Milankovitch theory identifies three types of variation in the Earth's orbit around the Sun which could act as mechanisms to change the global climate. These include changes in the tilt of the Earth's axis (obliquity), changes in the shape of Earth's orbit (eccentricity) and the shifting of the equinoxes (precession) (Berger 1960, Idnurm and Cook 1980, Watts 1984, Berger 1988, Broecker 1992, Imbrie *et al* 1993). Generally on the macroscopic scale, effect of the rotation of earth becomes substantially significant; motion of air in the atmosphere, flight of an aeroplane, path of a missile the and flow of air heated by the Sun are affected by the rotation of the Earth. Effect of the rotational force on the heated air is the cause of the tropical cyclones that exist on earth (Mitteilungen 1972, Prange 1994, Liang and Chan 2005, Haugland 2009). Tropical Cyclones move in counter-clockwise in the northern hemisphere but clockwise in the southern hemisphere. These directions of motion is due to the *inertia force* called *Coriolis force*. More importantly is the effect of the Coriolis force on the climatic changes. Climatic changes occur as a result of the rotation of the Earth relatively to the flow of atmospheric air and water heated by the Sun. The Coriolis force is as significant as any other inertial force and viscous forces in the

---

[3] Author to whom any correspondence should be addressed.

basic flow equations and it is of comparable magnitude with other magnetohydrodynamic forces and has strong effect on hydromagnetic flow in earth's liquid core (Mitteilungen 1972, Deng *et al* 2017).

There have been increasing interests in the study of effect of Coriolis force and/or magnetic parameters on hydrodynamic flow over a (stretching/shrinking) sheet in the recent years due to its several applications in geophysical and astrophysical problems, fluid engineering, extrusion of a polymer in a melt spinning process, manufacturing of plastic films, wire drawing, hot rolling, centrifugal bioreactor, and glass fiber production (Mishra and Jena 2014, Suresh and Manglik 2014, Ali *et al* 2015). Mitteilungen (1972) analyzed the unsteady induced hydromagnetic convective free flow in a semi-infinite body of an incompressible fluid bounded by an infinite rigid body undergoing rotation with an angular velocity and investigated the simultaneous effects of Coriolis force and rotation on the hydromagnetic flow. Sarker (1997) theoretically studied the effect of Coriolis force on the vorticity covariance of magnetohydrodynamic turbulent flow of dusty incompressible flow and obtained a general set of equations to determine the vorticity covariance of magnetohydrodynamic dusty fluid turbulent flow in the presence of Coriolis force which agrees with literature where the Coriolis term is ignored. In a study by Hasan and Sanghi (2007), the role of Coriolis forces in two-dimensional thermally driven flows in rotating enclosures of an arbitrary cross section was examined theoretically. In their work, it is shown that the Coriolis force does not play any role in the evolution of the velocity and temperature fields in a circular rotating enclosure. Detzel *et al* (2009), in an experimental study, examined the laminar fluid flow profile in a plane normal to the axis of rotation in a canonical shaped continuous centrifugal bioreactor which results from the Coriolis effect on momentum transport due to reactor rotation. It was reported that the when reactor is rotated, vortices develop and the flow profile becomes dominated by Coriolis forces resulting in the majority of flow up the leading wall of the reactor as dye initially enters the chamber. Moreso, it was also found out that at a certain velocity, a flow pattern largely unchanged becomes more defined with the exception of vortices. Hussain *et al* (2017) investigated the combine effects of Hall current and rotation on unsteady MHD free convective heat and mass transfer flow of an electrically conducting, viscous, incompressible fluid over an accelerated moving vertical plate with ramped temperature and ramped surface concentration through porous medium. It was found out that rotational parameter has positive effect on primary velocity but a retarding effect on secondary velocity near the surface. Vortex equation and three-dimensional Navier–Stokes equations under the Coriolis force was analyzed for incompressible fluid by Lee *et al* (2017). Kumar (2018) pondered over a three-dimensional unsteady flow of Cu-water nanofluid along an oscillating vertical sheet with the effect of thermal radiation in rotating frame of reference where nanofluid and sheet are rotating in a unison manner with constant rotation. Physically, there are many surfaces that possess non-uniform thickness. The motion of fluids over these kinds of surfaces is quite different from that of

cone, cylinder and pyramid. For instance, motion of air on the upper surface of the pointed edge of an aircraft, on the bonnet of cars, suit the case of fluid flow over the upper surface of a paraboloid of revolution. Recently, this has led to a note on the significance of quartic autocatalysis chemical reaction on the flow of dusty fluid over an object with non-uniform thickness by Animasaun *et al* (2019). Other works on non-uniform thickness include Khan *et al* (2018), Hayat *et al* (2016b). Also, when viscous dissipation is inevitable, Afridi *et al* (2019) presented the motion of hybrid nanofluid over a thin needle. Moreso, in the presence of multiple slip effects and partial slip, the dynamics of gyrotactic microorganisms and gold nano-particles was modeled using Carreau model; see Koriko *et al* (2018), Raju *et al* (2018). After deep observation of the effects of Coriolis force, it is worth mentioned that there is no report on the significance of Prandtl number, buoyancy, and rotation on the motion of air over the upper surface of the pointed edge of an aircraft, and on the bonnet of cars. This is considered necessary because the Earth surface can be approximated as the upper horizontal surface of a paraboloid of revolution and the Earth is known to adjust its shape from oblate spheroid to oblate ellipsoid and then to a geoid as it revolves round the Sun.

1.2. Research questions

The aim of this study is to explore the effect of Coriolis force on boundary layer flow of Newtonian fluid over an upper horizontal surface of a paraboloid of revolution. This report provide answer to the following questions;

1. What is the effect of Coriolis force on the velocity field of air?
2. How does Coriolis force affects temperature distribution across the flow of air?
3. What is the influence of Coriolis force on shear stress between any two layers across the flow of air?
4. What is the relationship between Coriolis force and buoyancy force as in the case of Newtonian fluid flow?

2. Research methodology

Following the formulation of Hayat *et al* (2016b, 2019), Waqas *et al* (2019), the theory of boundary flow was considered suitable to unravel the dynamics of two-dimensional steady boundary layer flow of air on the upper surface of a horizontally stretching surface of paraboloid of revolution. Assuming the fluid and the body are in rigid body rotation about the *y*-axis with a uniform angular velocity Ω. The *x*-axis is taken along the sheet, the *y*-axis taken as perpendicular to the fluid flow and *z*-axis is normal to the *x*- and *y*-axes. A shown in figure 1, the flow is over the region $y \geqslant 0$.

2.1. Derivation of the inertial forces in a rotating frame

In a rotating frame of reference, two paths are observed; the intended path and the apparent path. The intended path is the true path but the trajectory seem to have been deformed by
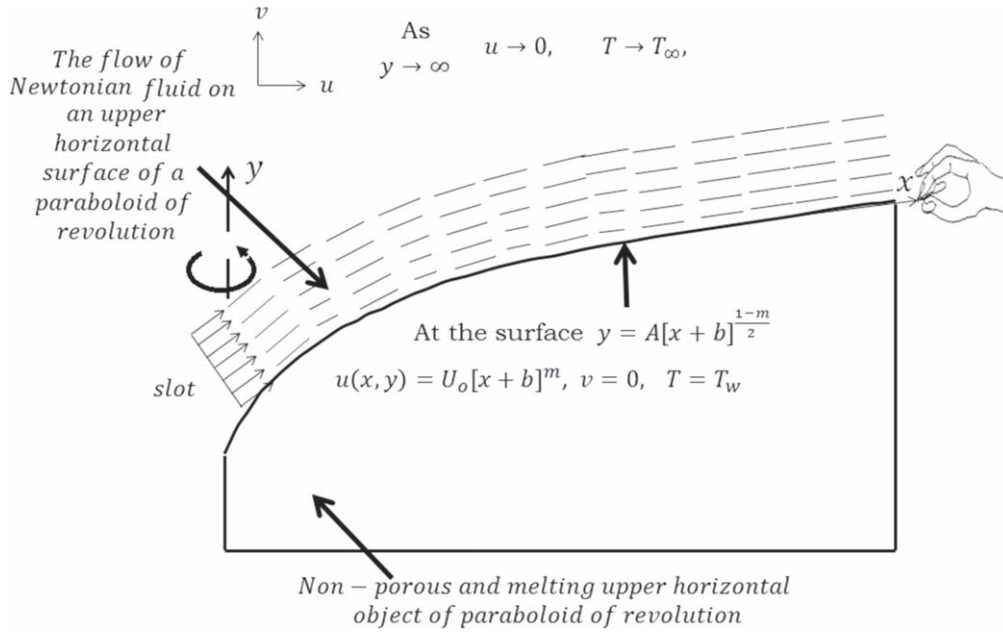
The flow of Newtonian fluid on an upper horizontal surface of a paraboloid of revolution

As

$y \to \infty$　　$u \to 0$,　　$T \to T_\infty$,

At the surface $y = A[x + b]^{\frac{1-m}{2}}$

$u(x, y) = U_o[x + b]^m$,　$v = 0$,　$T = T_w$

slot

Non − porous and melting upper horizontal object of paraboloid of revolution

Figure 1. Flow configuration.

some fictitious force, which is referred to as Coriolis force, which produce the apparent path. Expression for the Coriolis force will be derived in this section. Consider a frame of reference rotating at an angular velocity ω and let the position vector on the rotating frame be $r = (r_1, r_2, r_3)$. The absolute time derivative in the rotating frame is defined as

$$\frac{Dr}{Dt} = \frac{dr}{dt} + \omega \times r, \tag{1}$$

where $\frac{dr}{dt} = \left(\frac{dr_1}{dt}, \frac{dr_2}{dt}, \frac{dr_3}{dt}\right)$ is the apparent derivative with respect to the stationary frame which Newton's laws of motion apply to. To get the acceleration a_r in the rotating frame

$$a_r = \frac{D^2 r}{Dt^2} = \frac{D}{Dt}\left(\frac{Dr}{Dt}\right) = \frac{D}{Dt}\left(\frac{dr}{dt} + \omega \times r\right)$$

$$= \frac{d}{dt}\left(\frac{dr}{dt} + \omega \times r\right) + \omega \times \left(\frac{dr}{dt} + \omega \times r\right)$$

$$= \frac{d^2 r}{dt^2} + \frac{d}{dt}(\omega \times r) + \omega \times \frac{dr}{dt} + \omega \times (\omega \times r)$$

$$= \frac{d^2 r}{dt^2} + \frac{d\omega}{dt} \times r + \omega \times \frac{dr}{dt} + \omega \times \frac{dr}{dt} + \omega \times (\omega \times r)$$

$$= a + \frac{d\omega}{dt} \times r + 2\omega \times \frac{dr}{dt} + \omega \times (\omega \times r).$$

a_r is the absolute acceleration of the body as it moves in the rotating frame and $a = \frac{d^2 r}{dt^2}$ is the acceleration relative to the inertial frame of reference which Newton's laws of motion apply to. Clearly, on multiplying through by m

$$ma_r = ma + m\frac{d\omega}{dt} \times r + 2m\omega \times \frac{dr}{dt} + m\omega \times (\omega \times r)$$

$$ma = ma_r - m\frac{d\omega}{dt} \times r - 2m\omega \times \frac{dr}{dt} - m\omega \times (\omega \times r).$$

$F_E = -m\frac{d\omega}{dt} \times r$ is the Euler's force, $F_C = -2m\omega \times \frac{dr}{dt}$ is the Coriolis force and $F_G = -m\omega \times (\omega \times r)$ is the Centrifugal force. Each of these three forces are inertia forces acting on a body traveling in a rotating frame. Euler's force (also called the Azimuthal force) acts parallel but opposite to the angular velocity. This force is needed to keep the body from falling away from the orbit. The Coriolis force acts outward and perpendicular to the angular velocity while the Centrifugal force acts radially outward from the axis of rotation of the rotating frame. It is the force that causes the Earth to adjusts its shape from sphere to spheroid such that the force of gravity is perpendicular to the surface of the Earth. The rotating system produces Coriolis force $2\underline{\Omega} \times \underline{V}$, where $\underline{V} = (u, v, w)$ is the velocity of the fluid. Upon using the order of magnitude suggested by Ludwig Prandtl, it is worth remarking that the convective acceleration term of the well-known momentum equation for the flow along *x*- and *y*-directions must be updated with

$$2\frac{\Omega w}{U_0(x + b)^{1-m}}, \text{ and } -2\frac{\Omega u}{U_0(x + b)^{1-m}}$$

respectively. This is justifiable since the surface is stretched with velocity $u = U_0(x + b)^m$.

2.2. Governing equations of the transport phenomenon

Considering the case in which the conversion of kinetic energy to internal energy is negligible in the flow (which is true for less viscous fluids such as air). Hence, viscous dissipation was ignored. From the ongoing, the boundary layer equation is therefore given as

$$\frac{\partial u}{\partial x} + \frac{\partial v}{\partial y} = 0, \tag{2}$$

$$u\frac{\partial u}{\partial x} + v\frac{\partial u}{\partial y} + 2\frac{\Omega w}{U_0(x+b)^{1-m}}$$
$$= \frac{\mu}{\rho}\frac{\partial^2 u}{\partial y^2} + \left(\frac{m+1}{2}\right)g\beta(T-T_\infty), \quad (3)$$

$$u\frac{\partial w}{\partial x} + v\frac{\partial w}{\partial y} - 2\frac{\Omega u}{U_0(x+b)^{1-m}}$$
$$= \frac{\mu}{\rho}\frac{\partial^2 w}{\partial y^2} + \left(\frac{m+1}{2}\right)g\beta(T-T_\infty), \quad (4)$$

$$u\frac{\partial T}{\partial x} + v\frac{\partial T}{\partial y} = \frac{\kappa}{\rho c_P}\frac{\partial^2 T}{\partial y^2}. \quad (5)$$

Subject to the boundary conditions

$$\text{at } y = A(x+b)^{\frac{1-m}{2}}: \quad u = U_0(x+b)^m,$$
$$v = 0, \ w = 0, \ T = T_w(x) \quad (6)$$

$$\text{as } y \to \infty: \ u \to 0, \ w \to 0, \ T \to T_\infty, \quad (7)$$

where μ is the coefficient of viscosity, ρ is the fluid density, g is the acceleration due to gravity, β is the coefficient of thermal expansion, T is the temperature of the fluid, c_p is the specific heat capacity, κ is the thermal conductivity and wall temperature $T_w = A(x+b)^{\frac{1-m}{2}}$. It is important to notice that the third term on the left hand side of equations (3) and (4) represents the Coriolis term and it is a body force alongside the gravity force (the second term on the right hand side of equations (3) and (4)). The Coriolis force is considered as a body force since it also acts on all parts of the fluid (see figure 1 for the flow configuration). The quantities of interest are the skin friction and the heat transfer rate along the *x*-direction and *z*-direction and defined as

$$C_{fx} = \frac{\tau_{wx}}{\rho\sqrt{\frac{m+1}{2}}U_w^2}, \quad C_{fz} = \frac{\tau_{wz}}{\rho\sqrt{\frac{m+1}{2}}U_w^2}, \quad \text{and}$$

$$N_{ux} = \frac{(x+b)q_w}{\kappa(T_w-T_\infty)\sqrt{\frac{m+1}{2}}}.$$

respectively. The shear stress τ_w (skin friction) along the upper horizontal surface of a paraboloid of revolution is defined as

$$\tau_{wx} = \mu\frac{\partial u}{\partial y}\bigg|_{y=A(x+b)^{\frac{1-m}{2}}} \quad \text{and} \quad \tau_{wz} = \mu\frac{\partial w}{\partial y}\bigg|_{y=A(x+b)^{\frac{1-m}{2}}}$$

and the heat flux q_w at the wall is defined following Ara *et al* (2019) as

$$q_w = -\kappa\frac{\partial T}{\partial y}\bigg|_{y=A(x+b)^{\frac{1-m}{2}}}.$$

The governing equation is rendered dimensionless by using the similarity variables

$$u = \frac{\partial \psi}{\partial y}, \quad v = -\frac{\partial \psi}{\partial x},$$

$$w(\eta) = U_0(x+b)^m h(\eta), \quad \theta = \frac{T-T_\infty}{T_w-T_\infty} \quad (8)$$

$$\psi = \left(\frac{2}{m+1}\right)^{\frac{1}{2}}(\nu U_0)^{\frac{1}{2}}(x+b)^{\frac{m+1}{2}}f(\eta),$$

$$\eta = y\left(\frac{m+1}{2}\frac{U_0}{\nu}\right)^{\frac{1}{2}}(x+b)^{\frac{m-1}{2}} \quad (9)$$

$$\frac{\partial \eta}{\partial x} = \left(\frac{m-1}{2}\right)y\left(\frac{m+1}{2}\frac{U_0}{\nu}\right)^{\frac{1}{2}}(x+b)^{\frac{m-3}{2}},$$

$$\frac{\partial \eta}{\partial y} = \left(\frac{m+1}{2}\frac{U_0}{\nu}\right)^{\frac{1}{2}}(x+b)^{\frac{m-1}{2}} \quad (10)$$

and imposing the condition that $T_\infty \approx 0$ on the energy equation, we have

$$f''' + f''f - \frac{2m}{m+1}(f')^2 - \frac{K}{m+1}h + Gr\theta = 0, \quad (11)$$

$$h'' + h'f - \frac{2m}{m+1}hf' + \frac{K}{m+1}f' + Gr\theta = 0, \quad (12)$$

$$\theta'' + Pr\,f\theta' - Pr\left(\frac{1-m}{m+1}\right)f'\theta = 0. \quad (13)$$

And the boundary conditions become

$$\text{at } \eta = \chi: \ f' = 1, \ f = \left(\frac{1-m}{m+1}\right)\chi, \ h = 0, \ \theta = 1, \quad (14)$$

$$\text{and as } \eta \to \infty: \ f' \to 0, \ h \to 0, \ \theta \to 0, \quad (15)$$

where

$$K = \frac{4\Omega}{U_0^2}, \quad Gr = \frac{g\beta(T_w-T_\infty)}{U_0^2(x+b)^{2m-1}},$$

$$Pr = \frac{\rho c_P \nu}{\kappa}, \quad \chi = A\left(\frac{m+1}{2}\frac{U_0}{\nu}\right)^{\frac{1}{2}}$$

are the rotational parameter, Grashof number, Prandtl number and thickness parameter respectively. In order to set the equations up for easy computation, transform the domain from $[\chi, \infty)$ to $[0, \infty)$ by setting $\zeta = \eta - \chi \Rightarrow \eta = \zeta + \chi$ so that

$$f(\eta) = f(\zeta+\chi) = F(\zeta), \quad h(\eta) = h(\zeta+\chi) = H(\zeta),$$
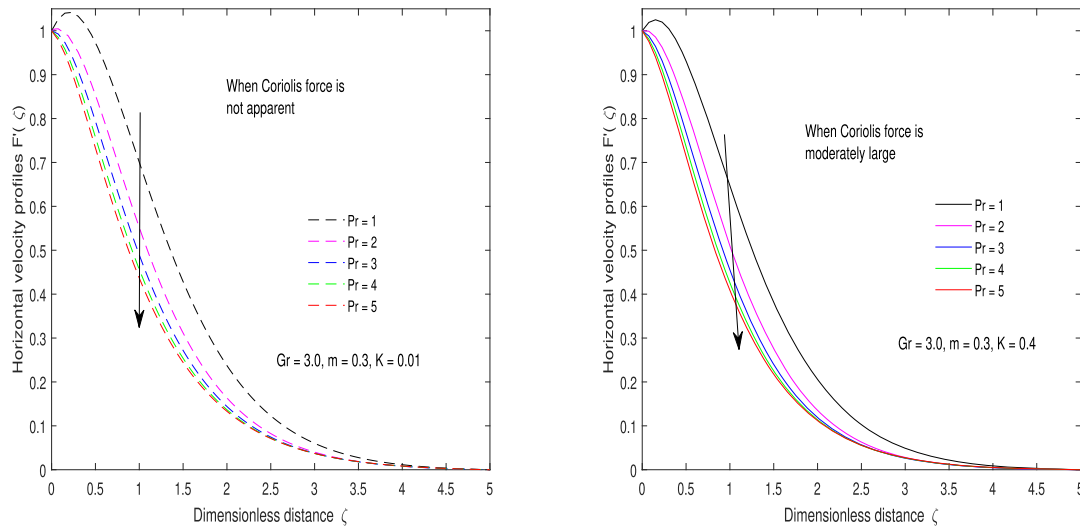$$\theta(\eta) = \theta(\zeta+\chi) = \Theta(\zeta).$$

The dimensionless equations are thus transformed to

$$F''' + F''F - \frac{2m}{m+1}(F')^2 - \frac{K}{m+1}H + Gr\Theta = 0, \quad (16)$$

$$H'' + H'F - \frac{2m}{m+1}HF' + \frac{K}{m+1}F' + Gr\Theta = 0, \quad (17)$$

$$\Theta'' + PrF\Theta' - Pr\left(\frac{1-m}{m+1}\right)F'\Theta = 0. \quad (18)$$

while the boundary conditions transform to

(a) Effect of Gr on horizontal velocity profiles when the
magnitude of rotation is small

(b) Effect of Gr on horizontal velocity profiles when
the magnitude of rotation is large

Figure 2. Effect of Prandtl number on horizontal velocity component of the flow.

at $\zeta = 0$: $\quad F' = 1, \;\; F = \left(\dfrac{1-m}{m+1}\right)\chi, \;\; H = 0, \;\; \Theta = 1$

(19)

as $\zeta \to \infty$: $F' \to 0, \;\; H \to 0, \;\; \Theta \to 0.$ (20)

The skin friction along the x and z axes transforms to

$$Re_x^{\frac{1}{2}} C_{fx} = F''(0) \quad \text{and} \quad Re_x^{\frac{1}{2}} C_{fz} = H'(0)$$

respectively and the Nusselt number transforms to

$$Re_x^{-\frac{1}{2}} N_{ux} = -\Theta'(0),$$

where the Reynold number Re_x is defined as

$$Re_x = \frac{U_w(x+b)}{\nu}.$$

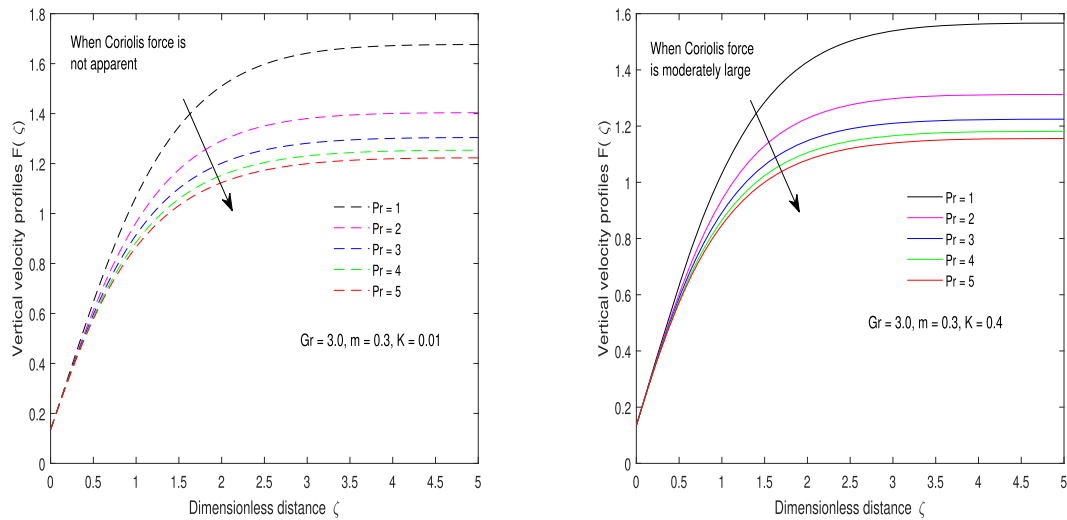## 3. Analysis and discussion of results

The equations governing the flow of Newtonian fluid over the upper horizontal surface of a paraboloid of revolution under the influence of Coriolis force were reduced to the system of equation (17) above and the resulting system of equations is solved using bvp5c MATLAB solver. Effects of each parameter (i.e. Grashof number (Gr), rotation parameter (K), velocity index m, and Prandtl number (Pr)) are investigated by observing what happens as the rotation is increased from very small to moderately large in order to understand the dynamics of flow and heat transfer processes. Solutions are illustrated graphically.

3.1. Effect of Prandtl number (Pr)

The effects of Prandtl number on the flow of Newtonian fluid over an upper horizontal surface of a paraboloid of revolution
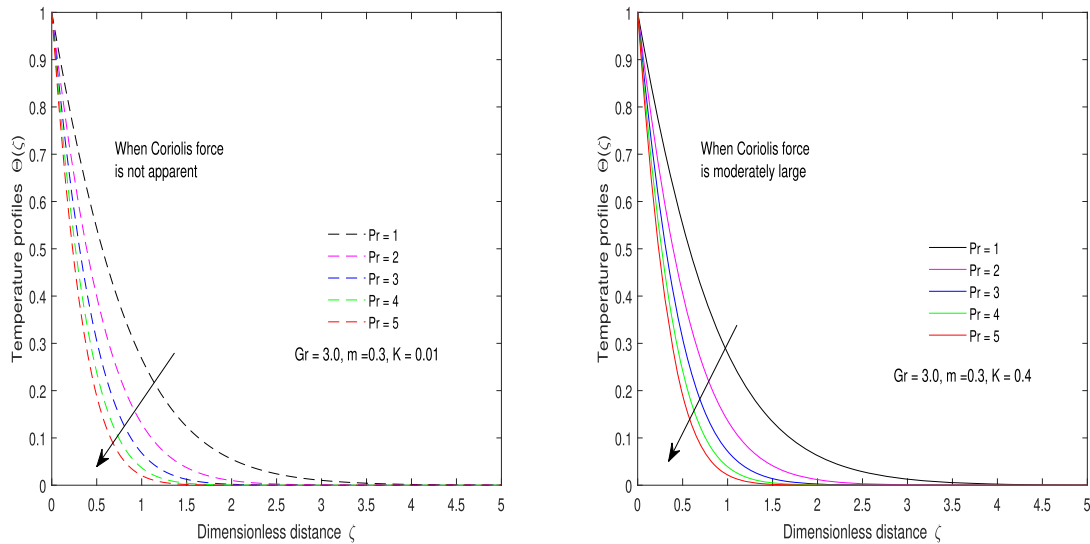
are investigated graphically at various levels of rotation (i.e. when rotation is moderately large, $K = 0.5$ and when rotation is not apparent, $K = 0.01$) and choosing $Gr = 3.0$, $m = 0.3$. It is observed that both the horizontal velocity function (F') and the vertical velocity function (F) decrease with Prandtl number (Pr) (see figures 2 and 3). Figure 4 reveals that the rate of change of temperature profile (Θ) decreases with increase in the Prandtl number (Pr). It is also discovered that the shear stress decreases near the upper horizontal surface of a paraboloid of revolution and increases at the free stream (see figure 5).

It is important to reiterate here that Prandtl number is measured as the ratio of the momentum diffusivity to the thermal diffusivity. From this definition, it is obvious that increase in the Prandtl number means decrease in the thermal diffusivity or increase in the momentum diffusivity, and consequently, convection is more responsible for the transfer of energy than heat diffusion. In order to investigate the effects of Prandtl number on the flow of Newtonian fluid over upper horizontal surface of paraboloid of revolution, graphs are plotted and taking $K = 0.4$ and 0.01, $m = 0.3$, $Gr = 3$ over the interval $0 \leqslant \zeta \leqslant 5$. As observed from figure 2, increase in the Prandtl number leads to a decrease in the horizontal and vertical velocities. As expected, decrease in heat diffusion should have negative influence on the velocities. Observe from figures 2(a) and (b) and figures 3(a) and (b) that peak of the horizontal and vertical velocities are high when the rotation is not apparent but low when the rotation is moderately large. Under the influence of a rotating frame, the system adjusts itself by expending some energy and thereby reducing the energy responsible for the dynamics of the flow. This result agrees with the result obtained by Hussain *et al* (2017). At high Prandtl number, momentum diffusivity dominates the flow (i.e. less heat is transferred). This agrees with figure 4 where temperature distribution decreases as Prandtl number increases. Observe that the shear stress

(a) Effect of Gr on vertical velocity profiles when the magnitude of rotation is small

(b) Effect of Gr on vertical velocity profiles when the magnitude of rotation is large

Figure 3. Effect of Prandtl number on vertical velocity component of the flow.

(a) Effect of Gr on temperature profiles when the magnitude of rotation is small

(b) Effect of Gr on temperature profiles when the magnitude of rotation is large

Figure 4. Effect of Prandtl number on temperature of the flow.
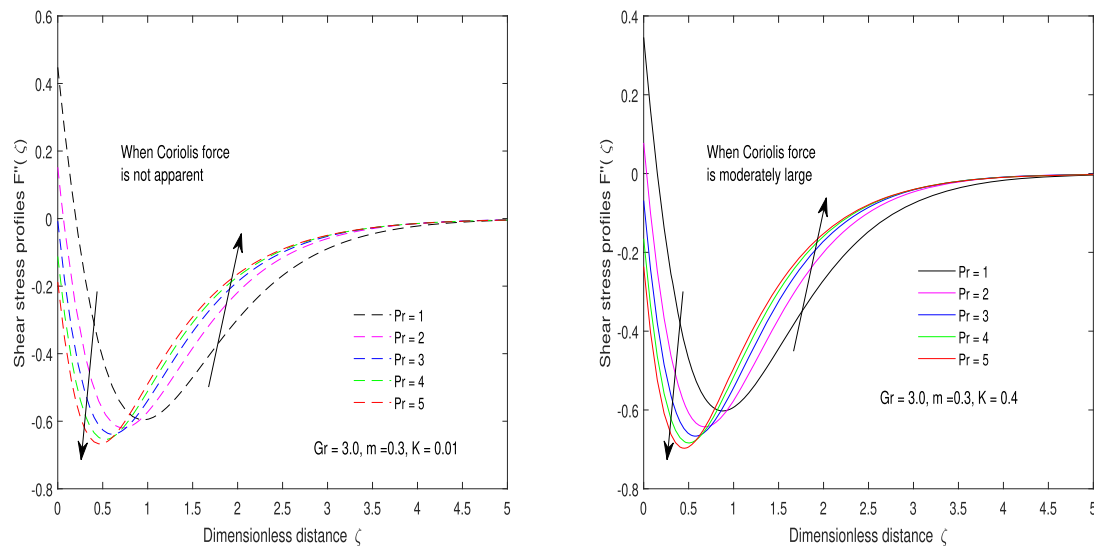
reaches the minimum when rotation is not apparent (compare figures 5(a) and (b)). Hence, as rotation increases, shear stress increases.

3.2. Effect of Grashof number (Gr)

The effects of thermal Grashof number on the flow of Newtonian fluid over an upper horizontal surface of a paraboloid of revolution are depicted graphically at various levels of rotation (i.e. $K = 0.5$ and $K = 0.01$) and choosing $Pr = 0.72$, $m = 0.3$. It is observed that both the horizontal velocity function ($F'(\xi)$) and the vertical velocity function (F) increase with Grashof number (Gr) (see figures 6 and 7. Figure 8 reveals that

the rate of change of temperature profile (Θ) decreases with increase in the Grashof number (Gr). It is also discovered that the shear stress decreases near the upper horizontal surface of a paraboloid of revolution and increases at the free stream (see figure 9)).

A theoretical study of the flow of Newtonian fluid is carried out by using a numerical experiments whose results are discussed in this section. Thermal Grashof number measures the difference between the wall temperature and the temperature at the free stream. It has been established in literature that an increase in the temperature difference enhances the buoyancy force. From the theoretical study of this flow, it is observed that increase in the difference between the wall

(a) Effect of Gr on shear stress profiles when the magnitude of rotation is small

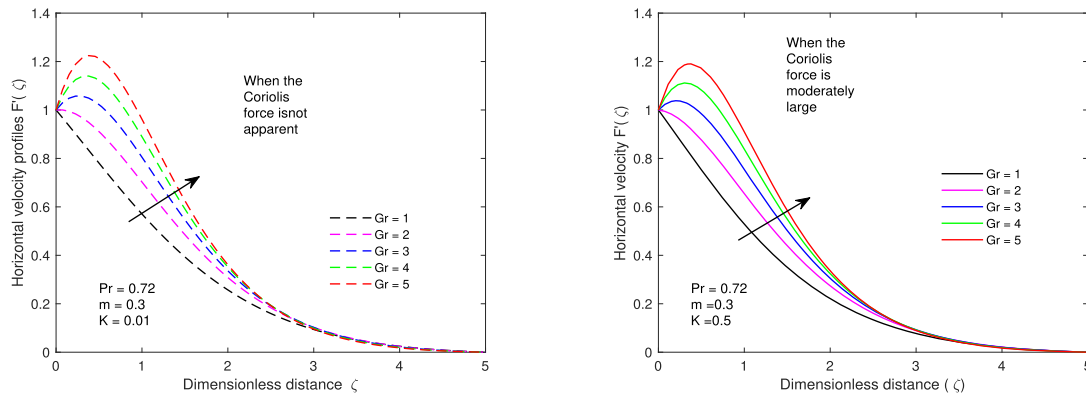(b) Effect of Gr on shear stress profiles when the magnitude of rotation is large

Figure 5. Effect of Prandtl number on shear stress of the flow.

temperature and free stream temperature (inadvertently, increase in the buoyancy force) results in an increase in the overall (horizontal and vertical) velocity of the flow. It is important to mention that the results of both Hussain *et al* (2017) and Zin *et al* (2017) agree with our result that horizontal and vertical velocities and temperature increase with increase in Grashof number. It is important to note that the effect of buoyancy is inhibited as rotation is gradually introduced. Observe from figures 6(a) and (b) and figures 7(a) and (b) that peak of the horizontal and vertical velocities are high when the rotation is not apparent but low when the rotation is moderately large. Under the influence of a rotating frame, the system will adjust itself by expending some energy and thereby reducing the energy responsible for the dynamics of the flow. It is observed that the rate of change of temperature profile decreases with increase in the Grashof number (Gr). The maximum temperature occurs at the wall but reduces across the free stream (see figure 8). Also, the present result corroborates with the outcome of the study by Zin *et al* (2017). It is easy to remark by comparing figures 8(a) and (b) that the rate of decrease of temperature decreases as rotation of the frame is increased. It is well known that fluid particles from the wall, and obviously the hottest, migrate to replace those in the colder region of the free stream. The temperature evens out throughout the flow as this continues. As rotation sets in, some of the hot fluid parcels at the wall are forced to travel horizontally and thus, reducing the rate of transfer of heat upstream. This explains why the rate of decrease in the temperature profile decreases as rotation is increased. It is also observed that the shear stress decreases near the upper horizontal surface of a paraboloid of revolution and increases at the free stream (see figure 9). This is probably due to exchange of particles between the lower and upper layers of the fluid. As Grashof number increases (and consequently, the difference between the temperature at the wall and

temperature at the free stream), the hot fluid particles near the wall rise rapidly and consequently decreasing the shear stress as observed in figure 9 near the wall. The decrease halts after some time and the shear stress starts to increase again. The shear stress increases at the free stream since the particles at the free stream are have less kinetic energy. In essence, increase in the Grashof number reduces the friction between layers close to the wall but the upper layers maintain high friction. When rotation is not apparent, it is observed that shear stress reaches a minimum at $(1.136, -0.6915)$ but at moderately large rotation, shear stress reaches a minimum at $(1.086, -0.6745)$. Hence, as buoyancy force increases and rotation increases, shear stress gets smaller. These results are in good agreement with the observation at the end of meta-analysis on the effects of Grashof number; see Animasaun *et al* (2018).

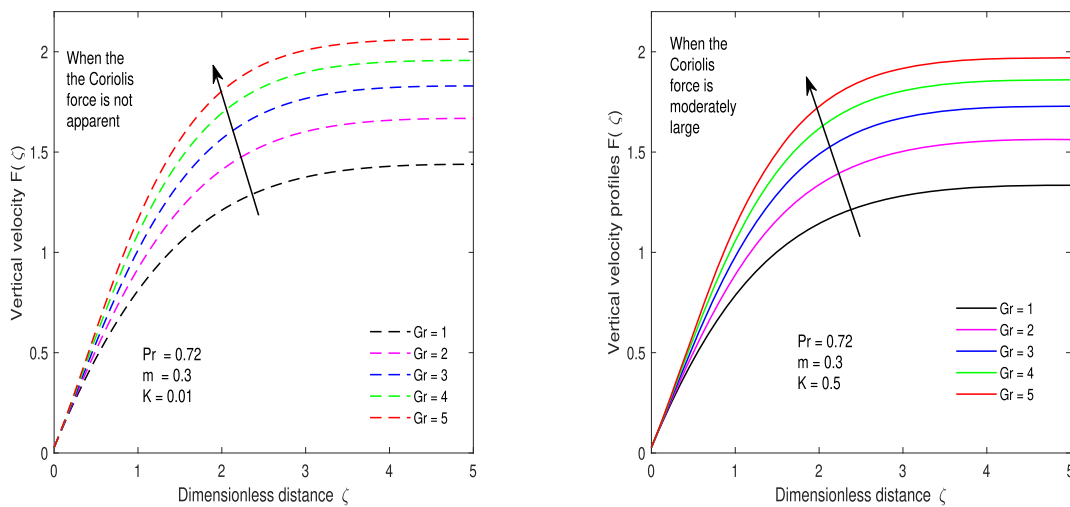### 3.3. Effect of velocity index (m)

In order to investigate the effects of velocity index on the flow of Newtonian fluid over upper horizontal surface of paraboloid of revolution, graphs are plotted while taking $K = \{0.4, \; 0.01\}$, $Pr = 0.72$, $Gr = 3$ over the interval $0 \leqslant \zeta \leqslant 5$. As observed from figure 10, horizontal velocity (F') increases with increase in velocity index. Vertical velocity decreases with increase in the velocity index (see figure 11). It is observed that the temperature profile (Θ) increases with increase in the velocity index (m) (see figure 12). It is observed that the shear stress decreases very fast at a region very close to the upper horizontal surface of a paraboloid of revolution (i.e. $\zeta < 0.25$ when $K = 0.01$ as shown in figure 13(a) and $\zeta < 0.15$ when $K = 0.5$ as shown in figure 13(b)). Furthermore, it is also revealed that the shear stress increases in the regions $0.4 < \zeta < 1.7$ and $0.2 < \zeta < 1.4$ when $K = 0.01$ (as shown in figure 13(a)) and when

(a) Effect of Gr on horizontal velocity profiles when the magnitude of rotation is small

(b) Effect of Gr on horizontal velocity profiles when the magnitude of rotation is large

Figure 6. Effect of thermal buoyancy on horizontal velocity component of the flow.

(a) Effect of Gr on vertical velocity profiles when the magnitude of rotation is small
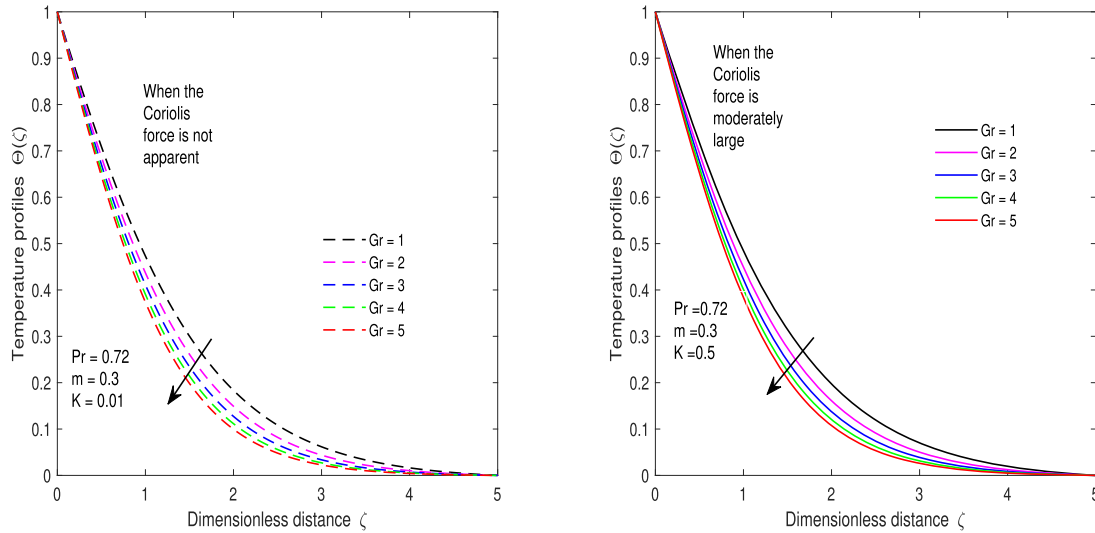
(b) Effect of Gr on vertical velocity profiles when the magnitude of rotation is large

Figure 7. Effect of thermal buoyancy on vertical velocity component of the flow.

$K = 0.5$ (as shown in figure 13(b)) respectively. As the flow gets into the free stream, the shear stress decreases ($\zeta > 1.8$ when $K = 0.01$ as shown in figure 13(a) and $\zeta > 1.6$ when $K = 0.5$ as shown in figure 13(b)).

Increase in the velocity index implies a decrease in the initial steepness of the surface and decrease in the vertical distance of the surface from the horizontal axis whereas a decrease in the velocity index implies decrease in the initial steepness and increase in the vertical distance of the surface from the horizontal axis. It is worth noting that as m increases from 0 to 1 the surface is changed from a paraboloid surface to a flat surface. In order to investigate the effects of velocity index on the flow of Newtonian fluid over upper horizontal surface of paraboloid of revolution, graphs are plotted and taking $K = 0.4$ and 0.01, $Pr = 0.72$, $Gr = 3$ over the interval $0 \leqslant \zeta \leqslant 5$. As observed from figure 10, horizontal velocity (F') increases with increase in the velocity index. The steepness reduces as the velocity index increases and consequently, there is reduction in the energy required to propel the flow a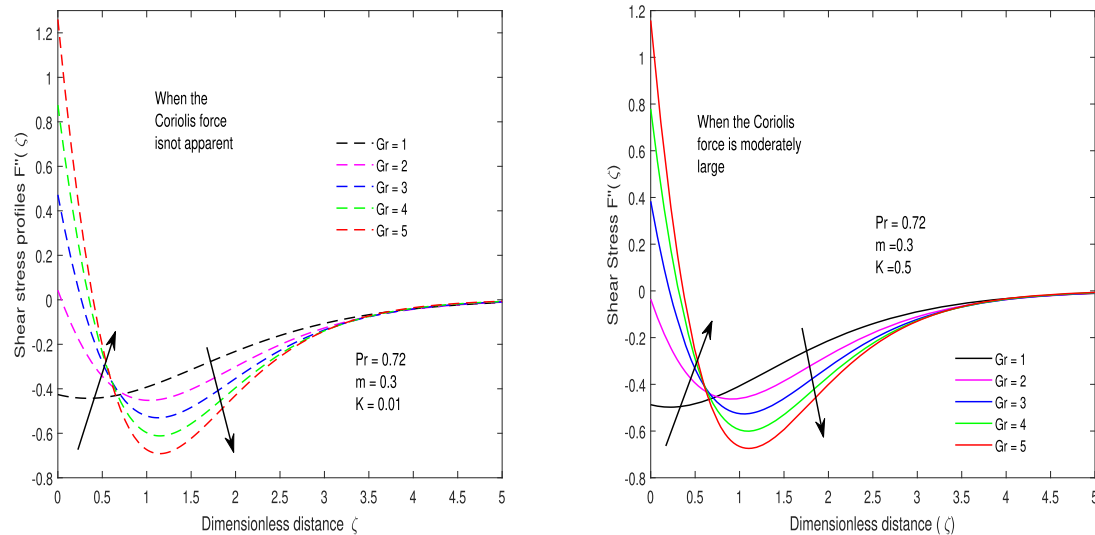cross the surface. Hence, the horizontal velocity increases with increase in the velocity index. Since flow is more favored horizontally, the vertical velocity component is adversely affected. This is as observed in figure 11. Notice also from figures 10(a) and (b) that the highest horizontal velocity is observed when rotation is not apparent. It can therefore be concluded that with increase in both rotation and velocity index, the horizontal velocity increases whereas increase in both rotation and velocity index causes a decrease in the vertical velocity (compare figures 11(a) and (b)). This result agrees with on the result obtained by Hussain *et al* (2017). Heat applied beneath the upper horizontal surface of a paraboloid of revolution passes through a nonuniform non-equal distance before truly reaching the surface where it is transmitted into the flow. This passage allows the dissipation of some of the heat energy, thereby reducing the amount of heat that eventually reaches the surface. Since increase in the velocity index reduces the initial steepness, then less energy is dissipated before touching the surface and thus leading to an increase in the temperature distribution in the flow. Figure 12 reveals that the

(a) Effect of Gr on temperature profiles when the magnitude of rotation is small

(b) Effect of Gr on temperature profiles when the magnitude of rotation is large

Figure 8. Effect of thermal buoyancy on temperature of the flow.

(a) Effect of Gr on shear stress profiles when the magnitude of rotation is small

(b) Effect of Gr on shear stress profiles when the magnitude of rotation is large

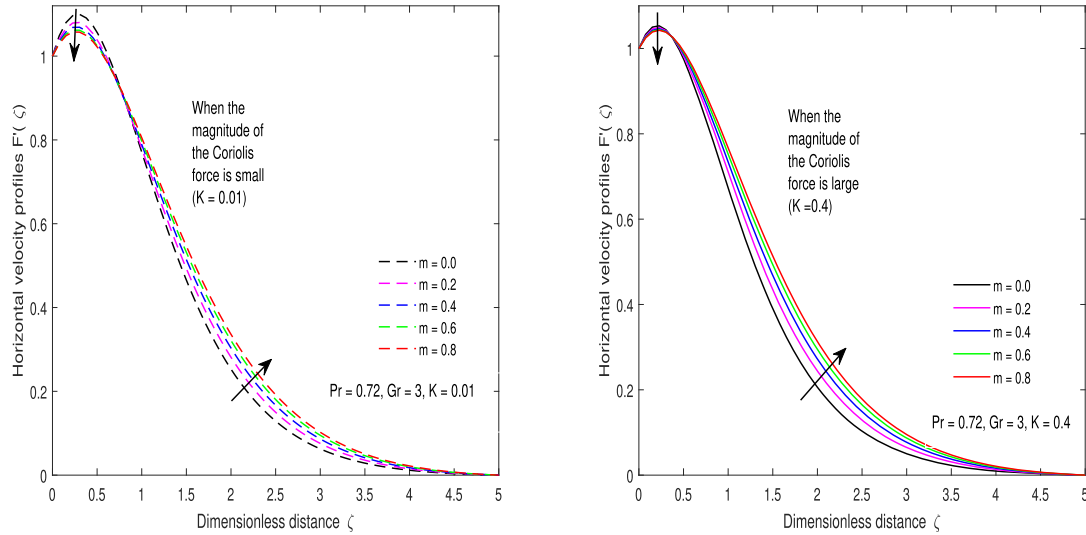**Figure 9.** Effect of thermal buoyancy on shear stress of the flow.

temperature profile (Θ) increases uniformly with increase in the velocity index (m). Observe that the shear stress reaches the maximum when rotation is not apparent (compare figures 13(a) and (b)). Hence, as rotation increases, shear stress decreases.

It is observed that the shear stress decreases very fast in the region next to the upper horizontal surface of a paraboloid of revolution (i.e. $\zeta < 0.25$ when $K = 0.01$ as shown in figure 13(a) and $\zeta < 0.15$ when $K = 0.5$ as shown in figure 13(b)). Furthermore, it is also revealed that the shear stress increases in the regions $0.4 < \zeta < 1.7$ and $0.2 < \zeta < 1.4$ when $K = 0.01$ (as shown in figure 13(a)) and when $K = 0.5$ (as shown in figure 13(b)) respectively. As the flow gets into the

free stream, the shear stress decreases ($\zeta > 1.8$ when $K = 0.01$ as shown in figure 13(a) and $\zeta > 1.6$ when $K = 0.5$ as shown in figure 13(b)).
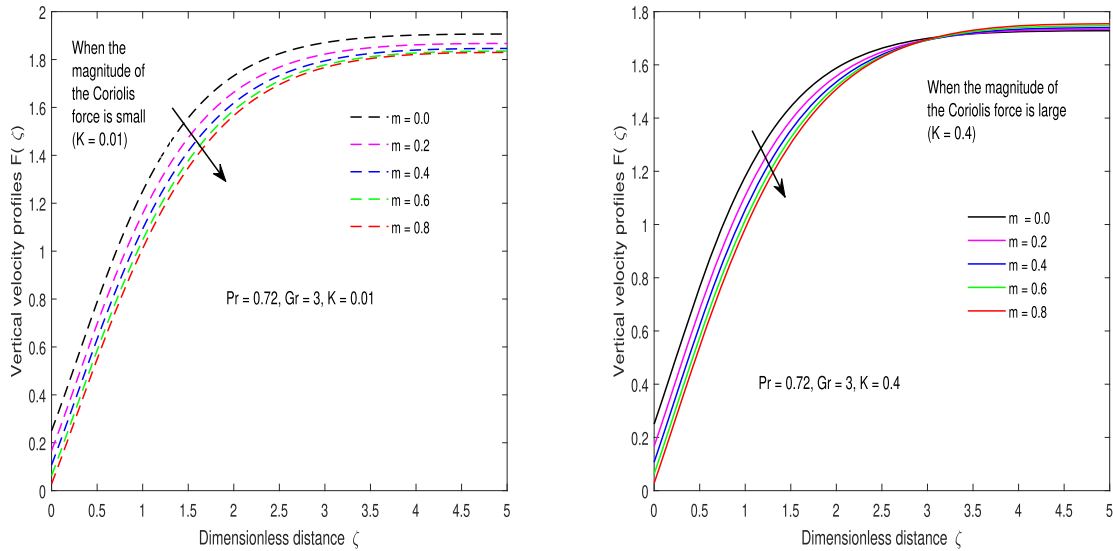
3.4. Effect of rotation parameter (K)

Effects of rotation parameter on the flow of Newtonian fluid over upper horizontal surface of paraboloid of revolution are investigated graphically by setting the parameters as $Gr = 3$, $Pr = 0.72$, $m = 0.3$ and $0 \leqslant \zeta \leqslant 5$. It is discovered that both the horizontal velocity (F') and the vertical velocity (F) decrease with increase in the rotation parameter (K) (figures 14(a) and (b)). The rate of change of temperature profile (Θ) increases with

(a) Effect of m on horizontal velocity when $K = 0.01$ (b) Effect of m on horizontal velocity when $K = 0.4$
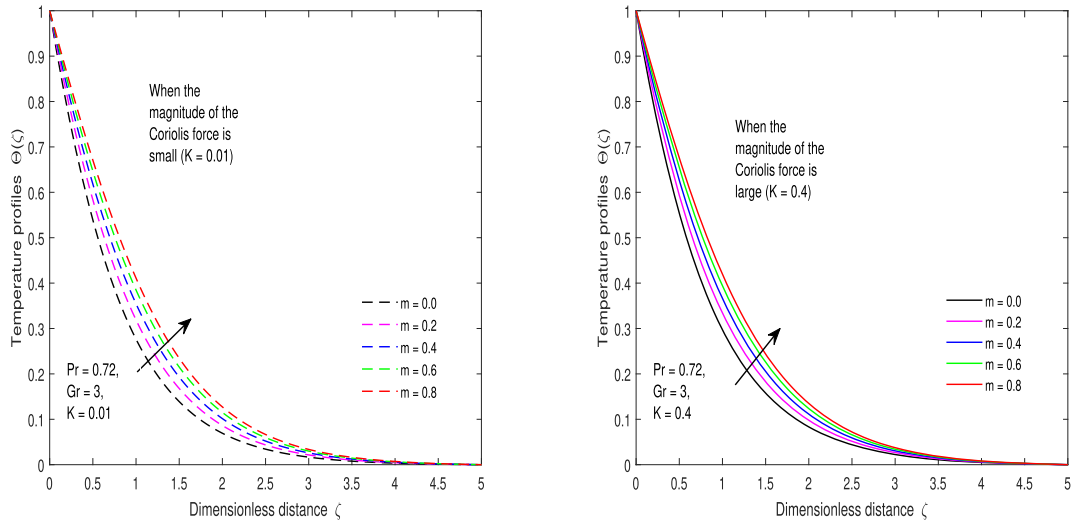
Figure 10. Effect of m on horizontal velocity.

(a) Effect of m on vertical velocity when $K = 0.01$ (b) Effect of m on vertical velocity when $K = 0.4$

Figure 11. Effect of m on vertical velocity.

increase in the rotation parameter (K) (see figure 15(a)). As shown in figure 15(b), the shear stress decreases near the upper horizontal surface of a paraboloid of revolution and increases at the free stream and figure 15(b) reveals that there is a turn in the effect within the interval $0.95 < \zeta < 1.03$. The shear stress decreases in the interval $0 \leqslant \zeta \leqslant 0.95$ and increases for $\zeta > 1.03$ into the free stream.
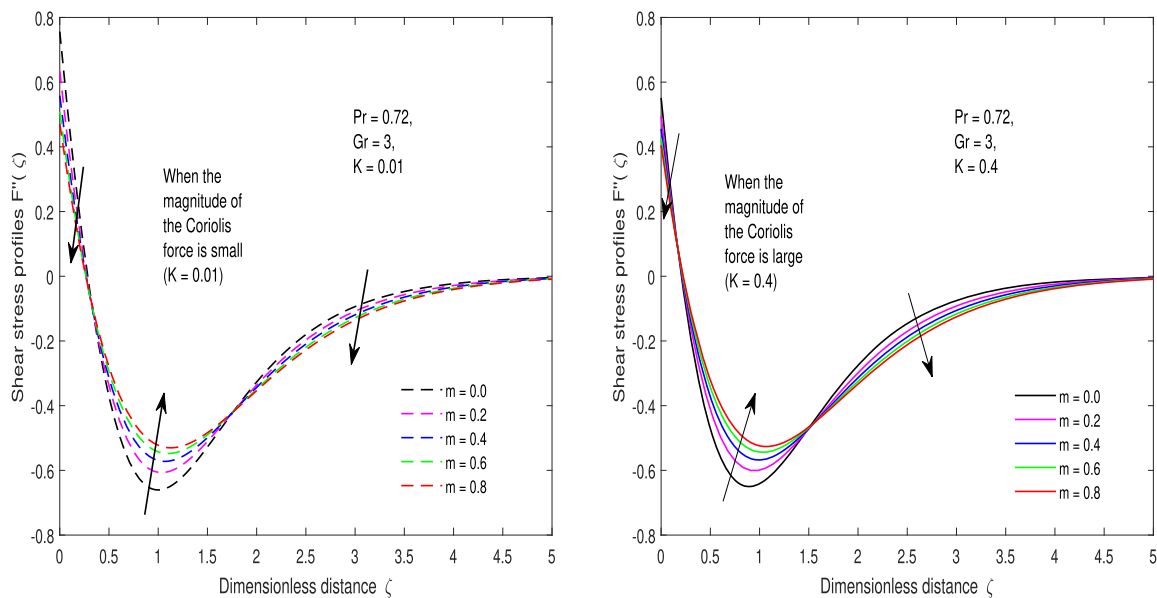
Effects of rotation parameter on the flow of Newtonian fluid over upper horizontal surface of paraboloid of revolution are investigated graphically, taking $Gr = 3$, $Pr = 0.72$, $m = 0.3$ and $0 \leqslant \zeta \leqslant 5$. It is worth noting that increase in the rotation parameter implies an increase in the magnitude of the uniform angular velocity and consequently increase in the Coriolis force. Some energy are dissipated to maintain the rotational motion and thereby having a negative effect on both

the vertical and horizontal velocities. This explains the observation in figures 14(a) and (b) where both the horizontal velocity (F') and the vertical velocity (F) decrease with increase in the rotation parameter (K). The dissipated energy is released in form of heat energy which increases the temperature of the system. This is the observation in figure 15(a) where the temperature profile (Θ) increases with increase in the rotation parameter (K). The result here is in agreement with the result of Seth *et al* (2010), Reddy *et al* (2016), Hussain *et al* (2017), Zin *et al* (2017). Due to the no-slip condition, it is expected that the effect of rotation will be more visible at the free stream, it is also observed that the shear stress decreases near the upper horizontal surface of a paraboloid of revolution $(0 \leqslant \zeta \leqslant 0.95)$ and increases at the free stream $(\zeta > 1.03)$. The interval $0.95 < \zeta < 1.03$ serves as the transition region.

(a) Effect of m on temperature profiles when $K = 0.01$ (b) Effect of m on temperature profiles when $K = 0.4$

Figure 12. Effect of m on temperature profiles.

(a) Effect of m on shear stress when $K = 0.01$ (b) Effect of m on shear stress when $K = 0.4$

Figure 13. Effect of m on shear stress.

3.5. Relationship between Grashof number and rotation parameter

The effect of both Grashof number and rotation parameter on the local skin friction and the Nusselt number are investigated. As shown in figure 16(a), at fixed rotational parameter, Nusselt number increases but increasing the rotation parameter tends to remove the increase caused by increasing Grashof number. Similar effect is also observed for the local skin friction. Increase in Grashof number at fixed rotational parameter causes an increases in the local skin friction but when rotation parameter increases, it tends to remove the rising effect caused by the increase in the Grashof number (see figure 17(a)). This implies that the effect of Grashof number and rotation parameter on the flow parameters are inversely related.

At fixed Grashof number, Nusselt number decreases slowly with the rotational parameter but increasing the Grashof number tends to remove the decrease caused by increasing rotational parameter (see figure 16(b)). Similar effect is also observed for the local skin friction. Increase in rotation parameter at fixed Grashof number a slow decrease in the local skin friction but increasing Grashof number tends to remove the slowly decreasing effect caused by the increase in the rotational parameter. This implies that the effect of Grashof number and rotation parameter on the flow parameters are inversely related (see figure 17(b)).
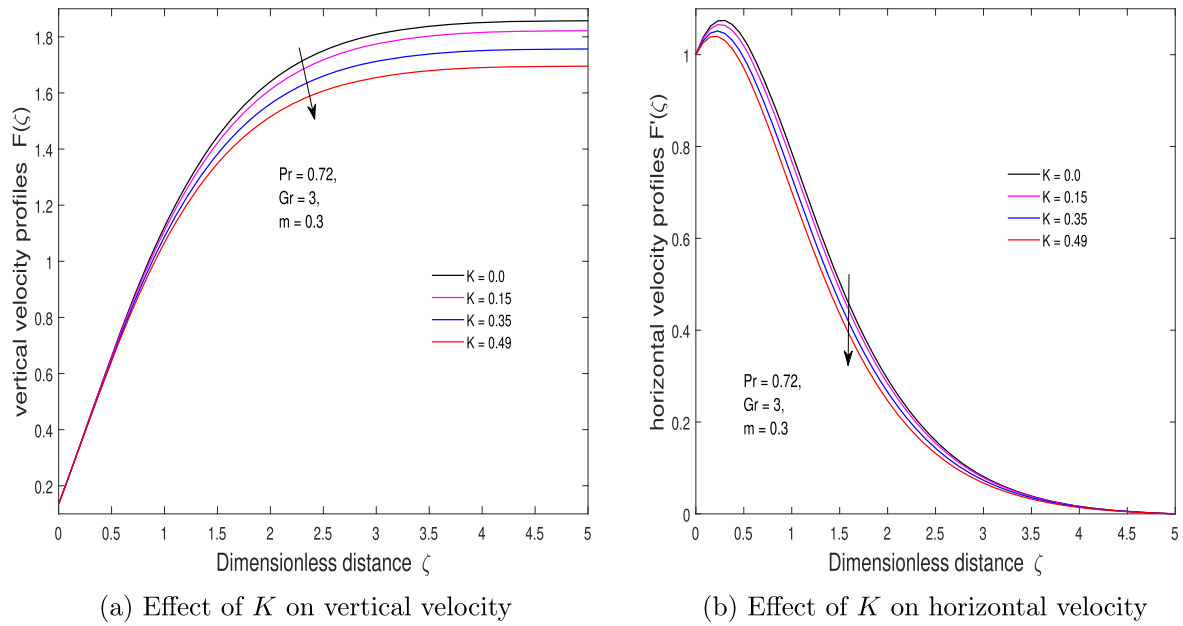
(a) Effect of K on vertical velocity

(b) Effect of K on horizontal velocity

Figure 14. Illustration of the effect of rotation parameter.

(a) Effect of K on temperature profiles

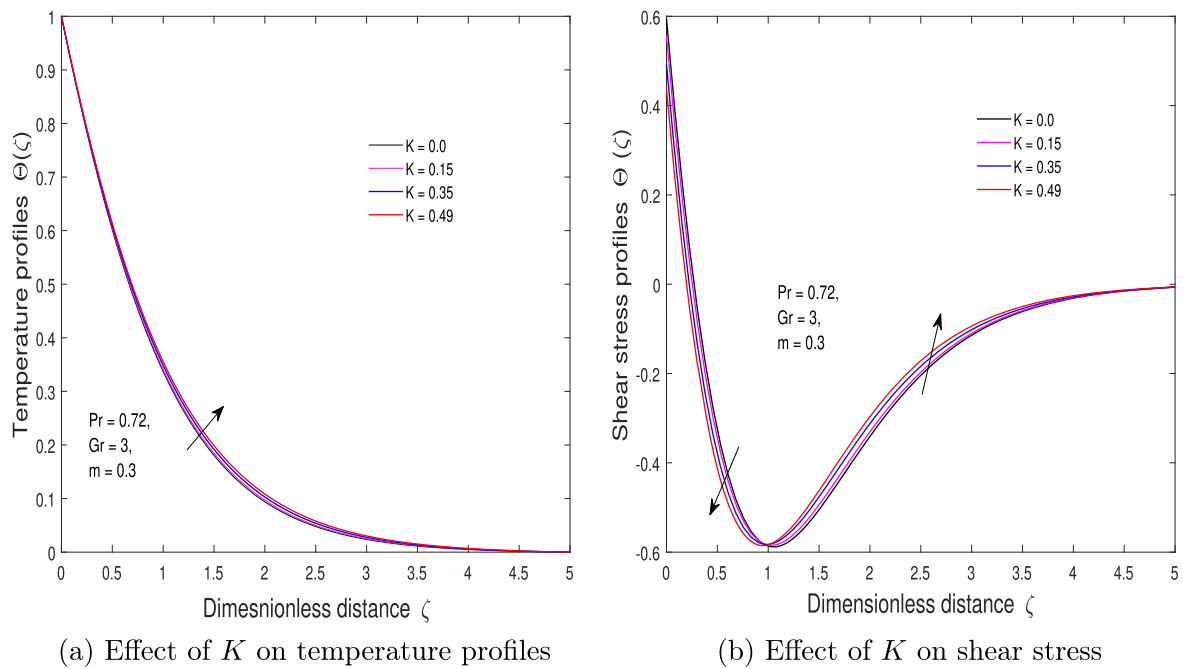(b) Effect of K on shear stress

Figure 15. Illustration of the effect of rotation parameter.

4. Conclusion and future study

The boundary layer flow of Newtonian fluid over the upper horizontal surface of a paraboloid of revolution in a rotating frame is investigated. The equations governing the flow is derived from the Navier–Stokes equation by incorporating the Coriolis force to cater for the force induced on the flow by the rotating frame. The resulting system of nonlinear partial differential equations is non-dimensionalised using the similarity variables and a system of nonlinear ordinary differential equations is obtained. The new system is then solved using the MATLAB bvp4c solver and the results are investigated. It

is observed that in a flow where convection is dominant (i.e. high Prandtl number), there is a decrease in the horizontal and vertical velocities and there is an increase in the temperature distribution. In a convective-dominant flow where rotation is increasing moderately, the peak of the horizontal and vertical velocities reduces while the shear stress increases. It is also observed that increase in the buoyancy force (i.e. Grashof number) has an increasing effect on theoverall (horizontal and vertical) velocity of the flow and temperature distribution. It is observed that the effect of buoyancy is inhibited as rotation is increasing moderately so that the peak of the horizontal and vertical velocities are found when buoyancy is high but
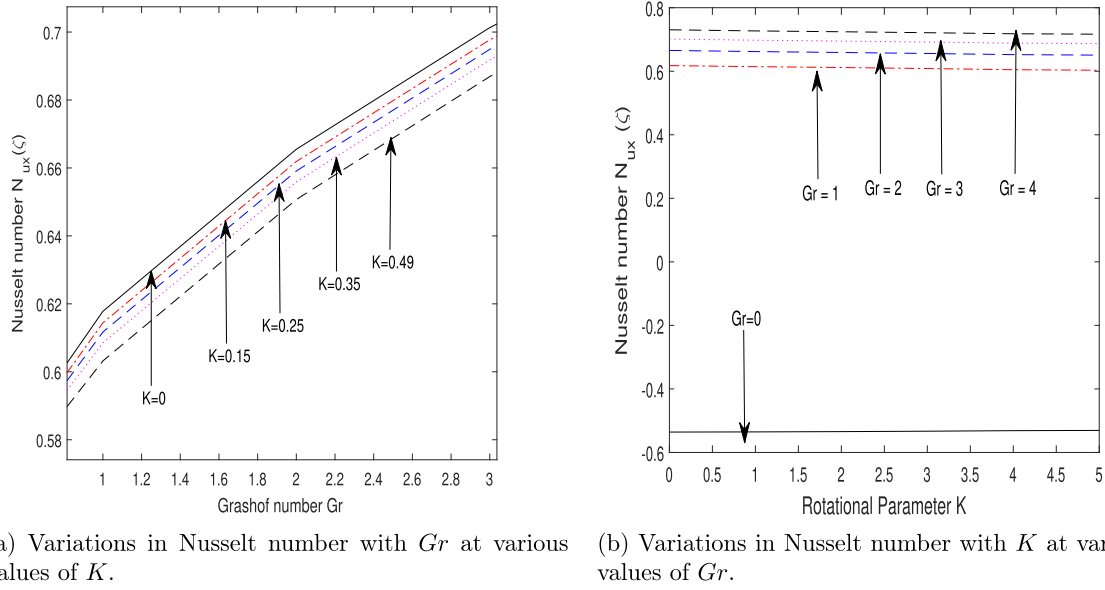
(a) Variations in Nusselt number with Gr at various values of K.

(b) Variations in Nusselt number with K at various values of Gr.

Figure 16. Variations in Nusselt number.

(a) Variations in Shear stress with Gr at various values of K.

(b) Variations in Shear stress with K at various values of Gr.
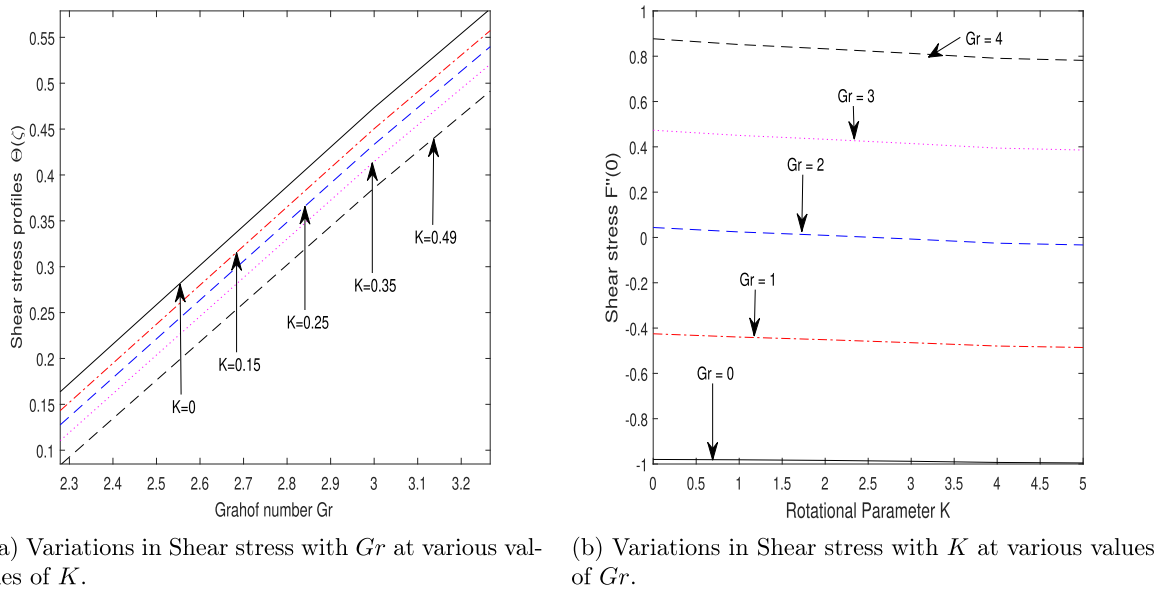
Figure 17. Variations in shear stress.

rotation is low. More so, the minimum shear stress is obtained at high rotation. As the surface over which the flow occurs changes from a paraboloid to a flat surface (i.e. increase in the velocity index), it is observed that the horizontal velocity and temperature distribution increases while the vertical velocity decreases. In fact, it is observed that increasing rotation enhances the effect of velocity index. That is, at high m and high rotation, the horizontal velocity increases the more while the vertical velocity decreases the more. As the velocity index increases and rotation also increases, shear stress decreases. It is observed that when all other flow parameters are kept fixed and rotation is increased, the horizontal velocity (F') and the vertical velocity (F) decrease, temperature distribution increases, and the shear stress decreases near the upper horizontal surface of a paraboloid of revolution while it increases at the free stream. The results of this study will help in the study of celestial objects (such as planets, moons, stars, galaxies, and comets etc.) and phenomena. The outcome of this study will also be useful in further explaining concepts such as the trade wind, gyres (ocean-circling currents), oceanic convergence and divergence, hurricane, tornadoes, etc. Further research can be done to investigate the flow of dusty air instead of pure air (as considered in this research), since air in the atmosphere usually carries some other tiny components.

Appendix. Boundary layer approximation

Consider the dimensionless distance η as the ratio of the vertical distance y to the boundary layer thickness δ i.e.

$\left(\eta = \frac{y}{\delta}\right)$ and

$$Re_x^{-\frac{1}{2}} \approx \frac{\delta}{x}, \quad x \sim L,$$

where L is the characteristic length of the horizontal wall on the upper horizontal surface of paraboloid of revolution defined as

$$L = \frac{2}{m+1}(x+b)^{1-m}.$$

Assuming velocity distribution in the boundary layer is similar to that of the dimensionless velocity so that $u \sim U_0$ and assuming the velocity may be expressed as a function of the similarity variable as

$$\frac{u}{U_0} = g(\eta) \Rightarrow u = U_0 g(\eta).$$

By the order of magnitude of the viscous term and the convective inertia term in the momentum equation

$$\frac{U_0^2}{L} \approx \nu \frac{U_0}{\delta^2} \;\Rightarrow\; \delta \approx \left(\frac{\nu L}{U_0}\right)^{\frac{1}{2}}$$

$$\Rightarrow \delta \approx \left(\frac{\nu}{U_0}\right)^{\frac{1}{2}}\left(\frac{2}{m+1}\right)^{\frac{1}{2}}(x+b)^{\frac{1-m}{2}}.$$

This suggests adopting the similarity variable

$$\eta = y\left(\frac{m+1}{2}\frac{U_0}{\nu}\right)^{\frac{1}{2}}(x+b)^{\frac{m-1}{2}}.$$

Introducing the stream function $\psi(x, y)$ so that the continuity equation is satisfied suggests to choose

$$u = \frac{\partial\psi}{\partial y}, \quad v = -\frac{\partial\psi}{\partial x}.$$

and thus

$$\psi = \int u \partial y = \int u \frac{\partial y}{\partial\eta}\mathrm{d}\eta = U_0\left(\frac{m+1}{2}\frac{U_0}{\nu}\right)^{-\frac{1}{2}}(x+b)^{\frac{m+1}{2}}$$

$$\times f(\eta), \quad \text{where } f(\eta) = \int g(\eta)\mathrm{d}\eta.$$

So that

$$\psi = \left(\frac{2}{m+1}\right)^{\frac{1}{2}}(\nu U_0)^{\frac{1}{2}}(x+b)^{\frac{m+1}{2}}f(\eta).$$

References

Afridi M I, Tlili I, Goodarzi M, Osman M and Khan N A 2019 Irreversibility analysis of hybrid nanofluid flow over a thin needle with effects of energy dissipation *Symmetry* **11** 663

Ali A O, Makinde O D and Nkansah-Gyekye Y 2015 Effect of hall current on unsteady mhd couette flow and heat transfer of nanofluids in a rotating system *Appl. Comput. Math.* **4** 232–44

Animasaun I L, Koriko O K, Mahanthesh B and Dogonchi A S 2019 A note on the significance of quartic autocatalysis chemical reaction on the motion of air conveying dust particles *Z. Nat.*

forsch. (A Journal of Physical Sciences) A **74** 879–904 (https://www.degruyter.com/view/j/zna.2019.74.issue-10/zna-2019-0180/zna-2019-0180.xml)

Ara A, Khan N A, Sultan F and Ullah S 2019 Numerical simulation of jeffery-hamel flow of bingham plastic fluid and heat transfer in the presence of magnetic field *Appl. Comput. Math.* **18** 135–48

Berger A 1960 The milankovitch astronomical theory of paleoclimates: a modern review *Vistas Astron.* **24** 103–22

Berger A 1988 Milankovitch theory and climate *Rev. Geophys.* **26** 624–57

Broecker W S 1992 Upset for milankovitch theory *Nature* **359** 779–80

Deng L, Li T, Bi M, Liu J and Peng M 2017 Dependence of tropical cyclone development on coriolis parameter: a theoretical model *Dyn. Atmos. Oceans*

Detzel C J, Thorson M R, Wie B J V and Ivory C F 2009 A study of the coriolis effect on the fluid flow profile in a centrifugal bioreactor *Biotechnol Prog.* **25** 1025–34

Hasan N and Sanghi S 2007 On the role of coriolis force in a two-dimensional thermally driven flow in a rotating enclosure *J. Heat Transfer* **129** 179–87

Haugland O A 2009 Cyclone on a turntable: illustrations of the coriolis force *Am. Assoc. Phys. Teach.* **47** 546–9

Hayat T, Aslam N, Khan M I, Khan M I and Alsaedi A 2019 Physical significance of heat generation/absorption and soret effects on peristalsis flow of pseudoplastic fluid in an inclined channel *J. Mol. Liq.* **275** 599–615

Hayat T, Khan M I, Farooq M, Alsaedi A, Waqas M and Yasmeen T 2016a Impact of cattaneo–christov heat flux model in flow of variable thermal conductivity fluid over a variable thicked surface *Int. J. Heat Mass Transfer* **99** 702–10

Hayat T, Khan M I, Farooq M, Yasmeen T and Alsaedi A 2016b Stagnation point flow with cattaneo-christov heat flux and homogeneous-heterogeneous reactions *J. Mol. Liq.* **220** 49–55

Hussain S, Jain J, Seth G S and Rashidi M M 2017 Free convective heat transfer with hall effects, heat absorption and chemical reaction over an accelerated moving plate in a rotating system *J. Magn. Magn. Mater.* **422** 112–23

Idnurm M and Cook P J 1980 Paleomagnetism of beach ridges in south australia and the milankovitch theory of ice ages *Nature* **286** 699–702

Imbrie J, Mix A C and Martison D G 1993 Milankovitch theory viewed from devils hole *Lett. Nat.* **363** 531–3

Khan M W A, Khan M I, Hayat T and Alsaedi A 2018 Entropy generation minimization (EGM) of nanofluid flow by a thin moving needle with nonlinear thermal radiation *Physica* B **534** 113–9

Koriko O K, Animasaun I L, Mahanthesh B, Saleem S, Sarojamma G and Sivaraj R 2018 Heat transfer in the flow of blood-gold carreau nanofluid induced by partial slip and buoyancy *Heat Transfer-Asian Res.* **47** 806–23

Kumar R 2018 Numerical exploration of thermal radiation and rotation effects on the 3-dimensional flow of cu-water nanofluid over an oscillating flat surface *Int. J. Appl. Comput. Math.* **4** 1–16 (https://link.springer.com/article/10.1007/s40819-017-0444-z)

Lee S, Ryi S-K and Lim H 2017 Solutions of navier-stokes equation with coriolis force *Adv. Math. Phys.* **2017** 1–9

Liang X and Chan J C 2005 The effects of the full coriolis force on the structure and motion of a tropical cyclone. I: Effects due to vertical motion *Am. Meteorol. Soc.* **62** 3825–30

Mishra S R and Jena S 2014 Numerical solution of boundary layer mhd flow with viscous dissipation *Sci. World J.* **2014** 1–5

Mitteilungen K 1972 On unsteady magnetohydrodynamic boundary layers in a rotating flow *ZAMM* **63** 623–6

Prange R 1994 Planet/magnetosphere/satellite couplings: observation from the Moon *Adv. Space Res.* **14** 183–92

Raju C, Hoque M M, Khan N A, Islam M and Kumar S 2018 Multiple slip effects on magnetic-carreau fluid in a suspension of gyrotactic microorganisms over a slendering sheet *Proc. Inst. Mech. Eng.* E **233** 254–66

Reddy J V R, Sugunamma V and Sandeep N 2016 Effect of nonlinear thermal radiation on mhd flow between rotating plates with homogeneous-heterogeneous reactions *Int. J. Eng. Res. Afr.* **20** 130–43

Sarker M S A 1997 Effect of coriolis force on vorticity covariance in mhd turbulent flow of dusty fluid *Int. J. Energy Res.* **21** 1399–403

Seth G S, Nandkeolyar R and Ansari M S 2010 Hartmann flow in a rotating system in the presence of inclined magnetic field with hall effects *Tamkang J. Sci. Eng.* **13** 243–52

Shah N A, Animasaun I L, Ibraheem R O, Babatunde H A, Sandeep N and Pop I 2018 Scrutinization of the effects of Grashof number on the flow of different fluids driven by convection over various surfaces *J. Mol. Liq.* **249** 980–90

Suresh M and Manglik A 2014 Mathematical analysis of hall effect on transient hartman flow about a rotating horizontal permeable surface in a porous medium under inclined magnetic field *Int. Scholarly Res. Not.* **2014** 1–8

Waqas M, Jabeen S, Hayat T, Khan M I and Alsaedi A 2019 Modeling and analysis for magnetic dipole impact in nonlinear thermally radiating carreau nanofluid flow subject to heat generation *J. Magn. Magn. Mater.* **485** 197–204

Watts R G 1984 A two-dimensional, seasonal, energy balance climate model with continents and ice sheets: testing the milankovitch theory *Tellus* **36A** 120–31

Zin N A M, Khan I, Shafie S and Alshomrani A S 2017 Analysis of heat transfer for unsteady mhd free convection flow of rotating jeffrey nanofluid saturated in a porous medium *Results Phys.* **7** 288–309